

# Rapid Microwave-Assisted Synthesis of Single-Crystalline Sb<sub>2</sub>Te<sub>3</sub> Hexagonal Nanoplates

Bo Zhou,<sup>†,\*</sup> Yong Ji,<sup>†</sup> Yu-Fei Yang,<sup>†</sup> Xing-Hua Li,<sup>†</sup> and Jun-Jie Zhu<sup>\*†</sup>

Key Laboratory of Analytical Chemistry for Life Science (MOE), School of Chemistry and Chemical Engineering, Nanjing University, Nanjing 210093, P.R. China, and Jiangsu Key Laboratory of Biofunctional Materials, College of Chemistry and Environmental Science, Nanjing Normal University, Nanjing 210097, P.R. China

Received December 1, 2007; Revised Manuscript Received April 15, 2008

**ABSTRACT:** A simple and rapid microwave-assisted wet chemical route was developed for the preparation of Sb<sub>2</sub>Te<sub>3</sub> hexagonal single-crystalline nanoplates with edge length of hundreds of nanometers. The products were characterized with X-ray powder diffraction (XRD), scanning electron microscope (SEM), transmission electron microscope (TEM), and selected area electron diffraction (SAED) techniques. The reaction mechanism was proposed and the effects of alkali, solvents, and stimulating factors such as ultrasonic wave and solvothermal process were studied. The effects of some additives were also discussed, and PVP (polyvinyl pyrrolidone) was found to be able to regularize and diminish the nanoplates.

## Introduction

Antimony telluride (Sb<sub>2</sub>Te<sub>3</sub>), a semiconductor with narrow band gap and layered structure, belongs to the V–VI class of materials, which are of special importance because of their thermoelectric (TE) properties. Possessing intrinsically a high figure-of-merit (ZT) because of its large Seebeck coefficient, this compound and its doped derivatives are considered to be the best candidates for near room-temperature TE applications.<sup>1</sup> At present, great attention is being paid to the nanostructured TE materials because both theoretical prediction and experimental investigation have suggested that the thermoelectric materials can be considered as a successful strategy to gain factorial enhancements in ZT due to both a high density of states and an increased phonon scattering or reduced lattice thermal conductivity in nanosystems.<sup>2–4</sup>

Sb<sub>2</sub>Te<sub>3</sub> was conventionally obtained via sintering the elements. Thin films were obtained by means of sputtering,<sup>5</sup> metalorganic chemical vapor deposition (MOCVD),<sup>6</sup> and flash evaporation.<sup>7</sup> More recently, Paul O'Brien and co-workers reported the preparation of Sb<sub>2</sub>Te<sub>3</sub> thin films from a single source precursor (SSP), Sb[(TePiPr<sub>2</sub>)<sub>2</sub>N]<sub>3</sub>, using the aerosol-assisted chemical vapor deposition (AACVD) process.<sup>8</sup> Milder electrodeposition was also used to obtain Sb<sub>2</sub>Te<sub>3</sub> thin films<sup>9</sup> and nanowire arrays.<sup>10</sup> However, the syntheses of Sb<sub>2</sub>Te<sub>3</sub> nanocrystals on a large scale via wet chemical route were rarely reported. Recently, Q. Wang et al.<sup>11</sup> and Shi et al.<sup>12</sup> hydrothermally synthesized Sb<sub>2</sub>Te<sub>3</sub> nanorods and nanobelts, respectively. On the other hand, although various chemical methods have been developed to prepare plate-like nanomaterials, these methods mainly focus on the fabrication of metal nanomaterials, such as Ag<sup>13–16</sup> and Au.<sup>17,18</sup> Wang and co-workers<sup>19</sup> described a 24 h long solvothermal reduction approach using NaBH<sub>4</sub> as a reductant to synthesize Sb<sub>2</sub>Te<sub>3</sub> nanoplates. And O'Brien et al.<sup>8</sup> obtained antimony telluride nanoplates in the temperature range 375–475 °C in their synthesis of Sb<sub>2</sub>Te<sub>3</sub> thin film. Such nanostructured materials are of particular interest for use in thermoelectric applications as they can give rise to a high figure-

of-merit. And it is therefore essential to develop an alternative approach to prepare a large quantity of nanosized single-crystalline Sb<sub>2</sub>Te<sub>3</sub> materials.

Herein, we report on a microwave-assisted wet chemical route based on the disproportionating reaction of Te to synthesize two-dimensional (2D) single-crystalline hexagonal nanoplates. The products were characterized with XRD, SEM, TEM, and SAED techniques. The reaction mechanism was proposed and the effects of some factors such as alkali, solvents, ultrasonic wave, and solvothermal process were studied. The effects of some additives were also discussed, among which PVP was found to be able to regularize and diminish the nanoplates. This work suggests a simple and rapid route for the synthesis of antimony telluride.

## Experimental Section

All reagents are of analytic purity and were used without further purification. The typical synthesis procedure is as follows: 2 mmol of antimony sodium tartrate (Na(SbO)C<sub>4</sub>H<sub>4</sub>O<sub>6</sub>), 3 mmol of Te powder, 2 g of NaOH, and 30 mL of ethylene glycol (EG) were added into a 100 mL round-bottomed flask, which was then put into a microwave oven equipped with a condenser to carry out the reaction under refluxing. The microwave frequency was 2.45 GHz, and the power was set at 280 W. The microwave irradiation time was 45 min. This time was prolonged to 2 h when polyvinyl pyrrolidone (PVP, K-30) was added into the reaction system to improve the morphology of the product. The product was cooled, centrifuged, washed with water and ethanol respectively several times, and then dried at 60 °C.

The products were characterized by X-ray powder diffraction (XRD) with a Philips X'pert X-ray diffractometer using Cu K $\alpha$  radiation ( $\lambda = 1.5418\text{\AA}$ ). The morphology and the microstructures of the products were investigated by transmission electron microscope (TEM) and selected area electron diffraction (SAED) with a JEM-200CX (JEOL, 200 kV) TEM, and a high-resolution transmission electron microscope (HRTEM, JEOL-2010). A JEOL-JSM-5610LV scanning electron microscope (SEM) was also used to obtain the products morphologies.

## Results and Discussion

**(A) Synthesis of Sb<sub>2</sub>Te<sub>3</sub> in the Absence of PVP.** Without the addition of PVP, pure Sb<sub>2</sub>Te<sub>3</sub> was obtained by microwave irradiating for 45 min as evidenced by the XRD pattern shown in Figure 1c. Each peak has the same position and the similar relative intensity as the corresponding diffraction peak of the rhomb-centered hexagonal Sb<sub>2</sub>Te<sub>3</sub> (JCPDS File. 71-0393).

\* Corresponding author. Tel.: 86-25-8359-4976. Fax: 86-25-8359-4976. E-mail: jjzhu@nju.edu.cn.

<sup>†</sup> Nanjing University.

<sup>‡</sup> Nanjing Normal University.

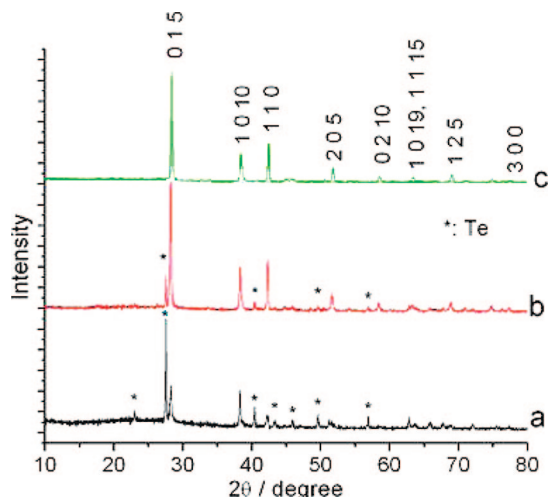
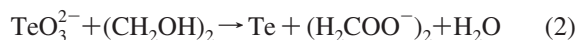
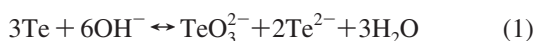


**Figure 1.** XRD patterns of the products obtained after (a) 10, (b) 25, and (c) 45 min of microwave-assisted reaction.

The result of the synthesis of Sb<sub>2</sub>Te<sub>3</sub> seemed similar to those of the synthesis of Bi<sub>2</sub>Te<sub>3</sub> reported previously.<sup>20</sup> However, further investigation indicated that the mechanism was different. The synthesis of Bi<sub>2</sub>Te<sub>3</sub> in EG was based on the polyol process, in which Bi(III) was first reduced by EG to metallic Bi, and then, this reduced Bi reacted with Te powder to produce Bi<sub>2</sub>Te<sub>3</sub>. But here, in the synthesis of Sb<sub>2</sub>Te<sub>3</sub>, no reduction of Sb(III) was observed. Figure 1a–c shows the XRD patterns of the products with reaction time of 10, 25, and 45 min, respectively. Before the reaction completion, besides Sb<sub>2</sub>Te<sub>3</sub>, only Te was observed, whose XRD peaks were in good agreement with those reported in the literature (JCPDS File No. 36-1452). And as reaction continues, this unreacted Te gradually decreased. However, no Sb was observed through the whole reaction process. Furthermore, if Te powder was not added into the reaction system, no solid metallic Sb was obtained. Obviously, the synthesis of Sb<sub>2</sub>Te<sub>3</sub> has another mechanism.

The mechanism may be expressed as follows:



First, in the alkali medium, Te disproportionates to TeO<sub>3</sub><sup>2-</sup> and Te<sup>2-</sup>, as represented in eq 1. Then, Te<sup>2-</sup> reacts with Sb<sup>III</sup> to produce Sb<sub>2</sub>Te<sub>3</sub>, as shown in eq 3. And the TeO<sub>3</sub><sup>2-</sup> is reduced by EG to Te in eq 2, which can disproportionate again. Though the disproportionation of Te (eq 1) is reversible, eqs 2 and 3 promoted it to move to the right, and led to the complete translation from Te to Te<sup>2-</sup>, from which Sb<sub>2</sub>Te<sub>3</sub> was then produced.

Two pieces of evidence support this mechanism. First, Te indeed can disproportionate in alkali medium as discussed previously.<sup>21,22</sup> And in this synthesis of Sb<sub>2</sub>Te<sub>3</sub>, a special purple color, the characteristic color of Te<sup>2-</sup> was observed in the solution, indicating the disproportionation of Te. Second, alkali can accelerate the reaction greatly. Reducing the amount of the NaOH added, the reaction slowed down obviously. And, without NaOH, almost no Sb<sub>2</sub>Te<sub>3</sub> was obtained.

Solvent is very important for this synthesis. Different solvents were tried in the experiments. In solvent of water, other reactions happened and no Sb<sub>2</sub>Te<sub>3</sub> was obtained. In ethanol, NaOH was almost insoluble, and no obvious reaction happened. A similar phenomenon was observed in dimethyl formamide (DMF),

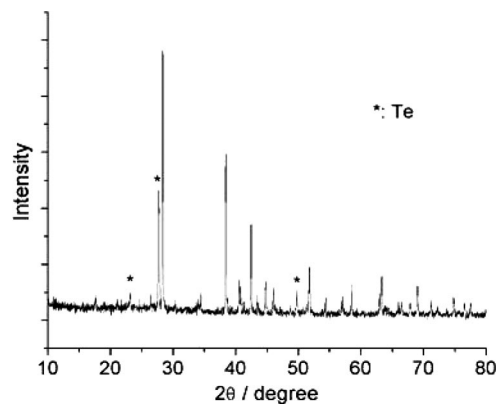


**Figure 2.** XRD pattern of Sb<sub>2</sub>Te<sub>3</sub> obtained after 48 h of solvothermal reaction.

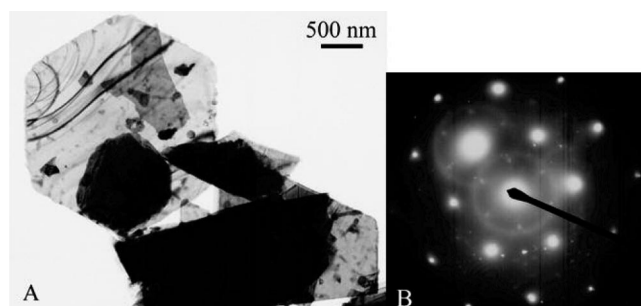


**Figure 3.** (A) TEM image and (B) SAED pattern of as-prepared Sb<sub>2</sub>Te<sub>3</sub>.

though the DMF is basic itself. The solubility of NaOH in the solvent, the reducibility and the boiling point (which limits the reaction temperature) of the solvent are all very important for the reaction as implied in the mechanism. The effect of the solvent confirms the above mechanism.

Microwave irradiation played an important role in this synthesis reaction. When the microwave irradiation was replaced by the ultrasonic irradiation, little Sb<sub>2</sub>Te<sub>3</sub> along with much unreacted Te were found in the product. It may be that sonication cannot supply enough stimulation. Lower reaction temperature is one of the reasons for this result. When similar reaction system was put into a Teflon-lined autoclave and solvothermally processed at 180 °C, which was little lower than the boiling-point of EG, similarly the microwave reaction temperature, ~197 °C, though Sb<sub>2</sub>Te<sub>3</sub> can be prepared, the reaction was much slower and not completed even after 48 h, as evidenced by the XRD pattern shown in Figure 2. Therefore, it is reasonable to suggest that microwave irradiation has special effects on the synthesis. No Sb peaks were found in Figure 2 as midproduct, demonstrating that the reaction mechanism is similar to that under microwave irradiation.

The as-prepared Sb<sub>2</sub>Te<sub>3</sub> were mainly plates with size of several μm, and some of them were hexagonal, as can be observed in the TEM image shown in Figure 3A. Interestingly, although the planar dimension is in micrometer scale, the plate is transparent under the electron beam, indicating that the plate is very thin. The selected area electron diffraction (SAED) pattern shown in Figure 3B also exhibits a hexagonal symmetry diffraction spot pattern. And the discrete and bright spots indicate the single-crystallinity of an individual plate.

**(B) Effect of PVP on the Synthesis of Sb<sub>2</sub>Te<sub>3</sub>.** In the synthesis, we tried to control the morphology of the product by

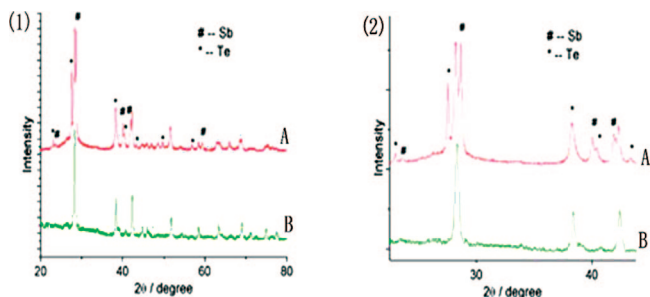
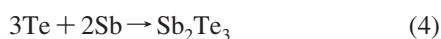


**Figure 4.** XRD patterns (in different magnification for (1) and (2)) of products obtained after reacted for (A) 1 h and (B) 2 h, with the addition of 0.5 g of PVP. The XRD peaks marked with “#” were in good agreement with those reported in the literature (JCPDS File No. 71–1173, hexagonal Sb). The XRD peaks marked with “\*” could be indexed to hexagonal Te (JCPDS File No. 36–1452).

adding hard or soft template. Te nanorods prepared as reported previously<sup>22</sup> were used as sacrificing templates, but no effect was observed. This was consistent with the mechanism: Te nanorods were dissolved at the early stage and could not serve as templates. The difference between the crystal structures of Te and  $\text{Sb}_2\text{Te}_3$  also made it hard to remain the original morphology. Although nonionic, anionic, and cationic surfactants, such as diethylene glycol (DEG), polyethylene glycol (PEG), sodium dodecyl sulfonate (SDS), and  $\beta$ -cyclodextrin, could be used as soft templates, they made no significant difference in the morphology, either.

However, the addition of polyvinyl pyrrolidone (PVP, K-30) made some differences. First, it slowed down the reaction. Second, it might change the reaction mechanism. Third, it made the products smaller and more regular.

From the XRD patterns shown in Figure 4, one can see that with the addition of PVP, the reaction was slowed down and not completed until reacted for 2 h. Before then, some Sb as well as unreacted Te was found in the products. The existence of Sb during the reaction and its final disappearance implied a different reaction mechanism: with the addition of PVP, which is reductive, Sb was reduced out and then reacted with Te to produce  $\text{Sb}_2\text{Te}_3$ , as represented in eq 4:



This direct reaction mechanism was discussed in detail elsewhere.<sup>23</sup>

Though the addition of PVP slowed down the reaction speed, the good dispersancy and high viscosity of the PVP solution made the products smaller and more regular as they grew gradually, because the mass transport was baffled. As shown in images A and B of Figure 5, a majority of the plates were hexagonal, and the edge length of the nanoplates reduced from several micrometers to 400–700 nm. The different amount of the PVP (0.1 or 0.5 g) added made a little difference in the morphology of the prepared  $\text{Sb}_2\text{Te}_3$  as shown in images A and B of Figure 5. However, as the reaction time was prolonged to 3 h, the nanoplates grew bigger to  $\sim 1 \mu\text{m}$  gradually (Figure 5C).

SEM images shown in Figure 6 confirmed TEM results. The  $\text{Sb}_2\text{Te}_3$  prepared with the addition of 0.5 g PVP and after 2 h of reaction were faceted hexagonal  $\text{Sb}_2\text{Te}_3$  nanoplates with edge length of 400–700 nm. The thicknesses of these nanoplates were  $\sim 80$  nm. The clear lattice fringes shown in Figure 6D indicate that the nanoplate is highly crystallized. The spacing of 0.213 nm corresponds to the (110) planes of  $\text{Sb}_2\text{Te}_3$ . The hexagonally symmetric spots in the SAED pattern indicate the single crystallinity and can be indexed on the basis of the rhombohedral  $\text{Sb}_2\text{Te}_3$ .

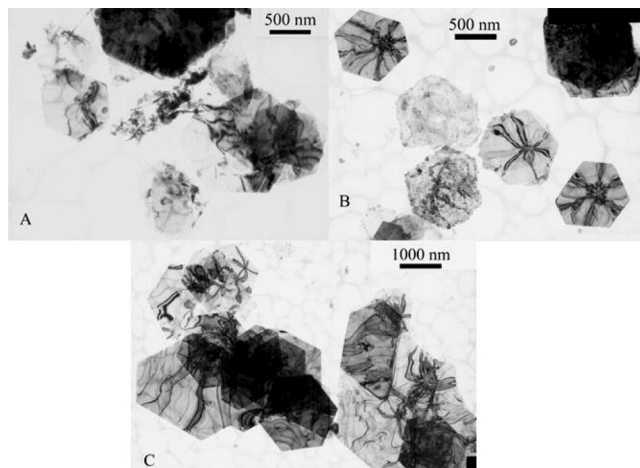


**Figure 5.** TEM images of  $\text{Sb}_2\text{Te}_3$  prepared with the addition of various amounts of PVP and after various reaction time: (A) 0.1 g of PVP, 2 h; (B) 0.5 g of PVP, 2 h; (C) 0.1 g of PVP, 3 h.

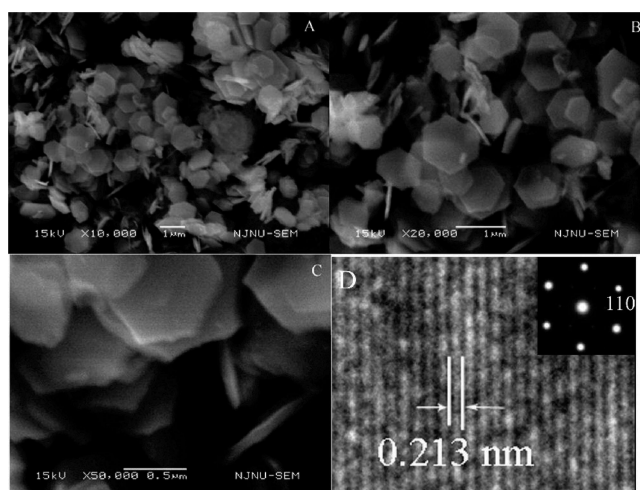


**Figure 6.** (A–C) SEM images in various magnifications of  $\text{Sb}_2\text{Te}_3$  prepared with the addition of 0.5 g of PVP and after 2 h of reaction; (D) HRTEM image and SAED pattern (the insert) of the same sample.

The formation of the faceted hexagonal  $\text{Sb}_2\text{Te}_3$  nanoplates might be due to the following two reasons. One is the intrinsic anisotropic layered crystal structure of  $\text{Sb}_2\text{Te}_3$ , which is the same to that of  $\text{Bi}_2\text{Te}_3$ .<sup>24</sup> A period of  $\text{Sb}_2\text{Te}_3$  crystal has 15 layers stacked along the  $c$ -axis and presents the combination of three hexagonal layer stacks of composition in which each set consists of five atoms ( $\text{Te}_1\text{—Sb—Te}_2\text{—Sb—Te}_1$ ). Between two adjacent  $\text{Te}_1$  layers, there are van der Waals bonds, while all others, covalent bonds. This special bonding structure leads to the faster growth of crystal along the top-bottom crystalline plane compared with that along the  $c$ -axis, which makes them tend to form platelike morphology.<sup>12</sup> The other is the selective adsorption of ions and small nanoparticles on the crystal faces during the growth.<sup>25</sup> This selective adsorption of small nanoparticles around the plates can be seen in the TEM image shown in Figure 5B. As the reaction time was prolonged, the small particles adsorbed around the plate were consumed to make the plate bigger.

## Conclusions

In summary,  $\text{Sb}_2\text{Te}_3$  hexagonal single-crystalline nanoplates with edge length of hundreds of nanometers were synthesized

via a simple and rapid microwave-assisted wet chemical route. Disproportionating reaction of Te played an important role in the synthesis of Sb<sub>2</sub>Te<sub>3</sub>, so alkali accelerated the reaction, and the solvents affected the reaction greatly because of the differences in the solubilization of NaOH, the reducibility, and the boiling point. Microwave irradiation was superior to ultrasonic wave and solvothermal process in this synthesis and made the reaction feasible and much faster. PVP was able to regularize and diminish the nanoplates, and it made a difference in the reaction mechanism.

**Acknowledgment.** This work is supported by the National Natural Science Foundation of China (Grants 20635020, 20575016, 90606016), NSFC for Creative Research Group (20521503), and the Natural Science Foundation of the Jiangsu Higher Education Institutions of China (Grant 06KJB150061).

### References

- (1) Venkatasubramanian, R.; Siivola, E.; Colpitts, T.; Quinn, B. O. *Nature* **2001**, *413*, 597–602.
- (2) Hicks, L. D.; Dresselhaus, M. S. *Phys. Rev. B* **1993**, *47*, 12727–12731.
- (3) Hicks, L. D.; Dresselhaus, M. S. *Phys. Rev. B* **1993**, *47*, 16631–16634.
- (4) Harman, T. C.; Taylor, P. J.; Walsh, M. P.; Laforge, B. E. *Science* **2002**, *297*, 2229–2232.
- (5) Romeo, N.; Bosio, A.; Tedeschi, R.; Romeo, A.; Canevari, V. *Sol. Energy Mater. Sol. Cells* **1999**, *58*, 209–218.
- (6) Giani, A.; Boulouz, A.; Delannoy, F. P.; Foucaran, A.; Boyer, A.; Aboulfarah, B.; Mzerd, A. *J. Mater. Sci. Lett.* **1999**, *18*, 541–543.
- (7) Patel, T. C.; Patel, P. G. *Mater. Lett.* **1984**, *3* (2), 46–50.
- (8) Garje, S. S.; Eisler, D. J.; Ritch, J. S.; Afzaal, M.; O'Brien, P.; Chivers, T. *J. Am. Chem. Soc.* **2006**, *128*, 3120–3121.
- (9) Leimkuhler, G.; Kerkamm, I.; Reineke-Koch, R. *J. Electrochem. Soc.* **2002**, *149*, C474–C478.
- (10) Jin, C. G.; Zhang, G. Q.; Qian, T.; Li, X. G.; Yao, Z. *J. Phys. Chem. B* **2005**, *109*, 1430–1432.
- (11) Wang, Q.; Jiang, C. L.; Yu, C. F.; Chen, Q. W. *J. Nanopart. Res.* **2007**, *9* (2), 269–274.
- (12) Shi, W. D.; Yu, J. B.; Wang, H. S.; Zhang, H. J. *J. Am. Chem. Soc.* **2006**, *128* (51), 16490–16491.
- (13) Chen, S.; Carroll, D. L. *Nano Lett.* **2002**, *2* (9), 1003–1007.
- (14) Yener, D. O.; Sindel, J.; Randall, C. A.; Adair, J. H. *Langmuir* **2002**, *18*, 8692–8699.
- (15) Maillard, M.; Giorgio, S.; Pileni, M.-P. *Adv. Mater.* **2002**, *14*, 1084–1086.
- (16) Hao, E.; Kelly, K. L.; Hupp, J. T.; Schatz, G. C. *J. Am. Chem. Soc.* **2002**, *124*, 15182–15183.
- (17) Simakin, A. V.; Voronov, V. V.; Shafeev, G. A.; Brayner, R.; Bozon-Verduraz, F. *Chem. Phys. Lett.* **2001**, *348*, 182–186.
- (18) Sun, X.; Dong, S.; Wang, E. *Angew. Chem., Int. Ed* **2004**, *43* (46), 6360–6363.
- (19) Wang, W.; Poudel, B.; Yang, J.; Wang, D. Z.; Ren, J. F. *J. Am. Chem. Soc.* **2005**, *127*, 13792–13793.
- (20) Zhou, B.; Zhao, Y.; Pu, L.; Zhu, J. J. *Mater. Chem. Phys.* **2006**, *96*, 192–196.
- (21) Zhou, B.; Zhang, J. R.; Zhao, L.; Zhu, J. M.; Zhu, J. J. *Ultrason. Sonochem.* **2006**, *13*, 352–359.
- (22) Zhou, B.; Zhu, J. J. *Nanotechnology* **2006**, *17* (6), 1763–1769.
- (23) Zhou, B.; Hong, J. M.; Zhu, J. J. *Chem. Lett.* **2008**, *37* (7), 730–731.
- (24) Lu, W.; Ding, Y.; Chen, Y.; Wang, Z. L.; Fang, J. J. *J. Am. Chem. Soc.* **2005**, *127*, 10112–10116.
- (25) Pileni, M. P. *Nat. Mater.* **2003**, *2*, 145–150.

CG7011815